Molecular Machines Hot Paper

Deutsche Ausgabe: DOI: 10.1002/ange.201502153
Internationale Ausgabe: DOI: 10.1002/anie.201502153

A Small Molecule Walks Along a Surface Between Porphyrin Fences That Are Assembled In Situ**

Sam Haq, Bareld Wit, Hongqian Sang, Andrea Floris, Yu Wang, Jianbo Wang, Lluïsa Pérez-García, Lev Kantorovitch, David B. Amabilino,* and Rasmita Raval**

Abstract: *An on-surface bimolecular system is described, comprising a simple divalent bis(imidazolyl) molecule that is shown to "walk" at room temperature via an inchworm mechanism along a specific pathway terminated at each end by oligomeric "fences" constructed on a monocrystalline copper surface. Scanning tunneling microscopy shows that the motion of the walker occurs along the [1$\bar{1}$0] direction of the Cu surface with remarkably high selectivity and is effectively confined by the orthogonal construction of covalent porphyrin oligomers along the [001] surface direction, which serve as barriers. Density functional theory shows that the mobile molecule walks by attaching and detaching the nitrogen atoms in its imidazolyl "legs" to and from the protruding close-packed rows of the metal surface and that it can transit between two energetically equivalent extended and contracted conformations by overcoming a small energy barrier.*

Walking molecules[1] have the potential to perform a variety of functions, from molecular transport and motility to energy conversion.[2] A key goal for artificial systems is confining molecular motion between two or more locations along a specified path. Biology achieves this with linear protein motor systems, such as myosin on actin or kinesin on microtubule filaments.[3] Surfaces are especially relevant environments to build and study molecular machines.[4] In particular, dynamic molecular systems that display motion along a given path on surfaces are of intense interest.[5] The non-directional[6] and unidirectional[7] motions of "molecular cars" on different surfaces are impressive achievements, with motion induced by stimuli. For surface-based molecular machines, important next steps include the creation of simple walking molecules that operate at room temperature and the confinement of motion within suitable surface frameworks.[8]

Herein, we show a bicomponent surface-based system wherein a simple molecular "walker" performs a directional walking motion by attachment and detachment at certain locations on a finite track akin to an inchworm mechanism.[3b] Furthermore, this directional motion can be effectively confined by construction of covalent molecular fences on the metal that are specifically oriented perpendicular to the path. In essence, the preferred path of the walker is now confined between two barriers, like an abacus.[9] In this type of system, at least two molecule-based components are necessary: One is immobile and acts as a confining barrier (the "fence") to the motion of the other molecule (the "walker"). The walker must move quickly and predominantly along one path dictated by specific interactions with an anisotropic single-crystal surface as illustrated in Figure 1 i.

The immobile component—the fence—was made from porphyrin **1** (Figure 1 ii), which forms covalent organometallic oligomers when heated on a Cu(110) surface, as demonstrated for analogous compounds.[10] Scanning tunneling microscopy (STM) shows that the distance between the neighboring monomeric units within the chain is 1.08 nm, which is consistent with covalent edge-to-edge porphyrin–Cu–porphyrin connections.[10] The fences run specifically along the corrugated [001] direction of the Cu surface[10] and are immobile at room temperature. The perpendicular [1$\bar{1}$0] direction of the surface consists of close-packed rows of copper atoms, which turned out to be an ideal path for the walker molecules to move along, as described below.

[*] Dr. S. Haq, B. Wit, Prof. R. Raval
Surface Science Research Centre
Department of Chemistry, University of Liverpool
Liverpool L69 3BX (UK)
E-mail: raval@liv.ac.uk

Dr. L. Pérez-García
Laboratori de Química Orgànica, Facultat de Farmàcia and Institut de Nanociència i Nanotecnologia, Universitat de Barcelona
08028 Barcelona (Catalonia, Spain)

Prof. D. B. Amabilino[+]
Institut de Ciència de Materials de Barcelona (CSIC)
Campus Universitari, 08193 Bellaterra (Catalonia, Spain)

Dr. A. Floris, Prof. L. Kantorovitch
Physics Department, King's College London, Strand
London, SE2 0LR (UK)
E-mail: lev.kantorovitch@kcl.ac.uk

H. Sang, Prof. Y. Wang, Prof. J. Wang
School of Physics and Technology, Center for Electron Microscopy and MOE, Key Laboratory of Artificial Micro- and Nano-structures
Wuhan University
Wuhan 430072 (China)

[+] Present address: School of Chemistry
The University of Nottingham
University Park, Nottingham NG7 2RD (UK)
E-mail: David.Amabilino@nottingham.ac.uk

[**] This research was supported by the UK EPSRC (EP/J019844/1 and EP/F00981X/1) and the MICINN (TEC2011-29140-C03-02). H.S., Y.W., and J.W. acknowledge financial support from the 973 Program (2011CB933300), the National Natural Science Foundation of China (11328403, 51271134, and J1210061), the Fundamental Research Funds for the Central Universities, and CERS-1-26 (China Equipment and Education Resources System).

Supporting information for this article is available on the WWW under http://dx.doi.org/10.1002/anie.201502153.

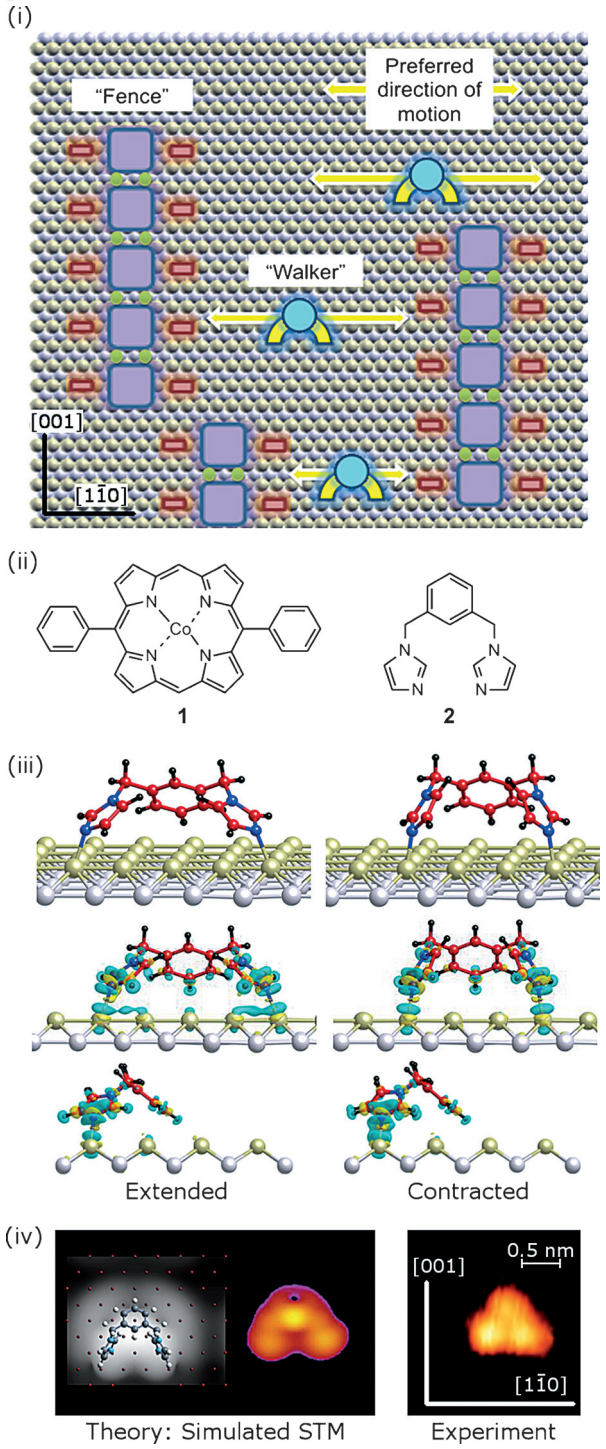

Figure 1. i) Representation of the system described here, in which a mobile molecule (the walker) shuttles between two immobile barriers (fences) along a preferred direction of diffusion owing to the anisotropy of the underlying single-crystal surface. ii) Cobalt diphenylporphyrin (**1**) and 1,3-bis(imidazol-1-ylmethyl)benzene (**2**), which form the immobile and mobile components of the system, respectively. iii) Two DFT-relaxed energetically equivalent geometries of the molecule on the surface with the feet held four (extended) and three (contracted) Cu atomic distances (a_0) apart shown as ball-and-stick models of the calculated geometries (top), and as the front (middle) and side views (bottom) of the structures with the charge density differences shown in yellow (excess) and green (depletion) at ± 0.003 atomic units. iv) Simulated STM image (1.0 V) of the contracted geometry and experimental STM image ($I(t) = -0.14$ nA, $V(t) = -710$ mV) of a single molecule on the surface.

Compound **2** (Figure 1 ii) was used as the walker molecule because it provided two particular attributes: First, it has the ability to bind to the surface with reasonable strength by specific molecule–Cu interactions; second, it possesses sufficient conformational flexibility to allow binding to surface atoms located at different separations, thus enabling the molecule to shift position without large energetic penalties. The walker has two "feet" that adhere specifically to the surface; here, the imidazolyl groups perform this function because the N atoms can adsorb specifically and reversibly to the Cu atoms in the top row of the surface. A degree of molecular flexibility is conferred by the methylene spacer in between the imidazolyl groups and the phenyl ring. In solution, this spacer allows for a horseshoe-shaped conformation when appropriate supramolecular interactions occur,[11] whereas in the solid state, the derivative's legs are usually splayed.[12] These observations confirmed the flexibility of the molecule, making it amenable for a walking-type motion. Specifically, the horseshoe conformation is ideal for binding to the surface via both imidazolyl feet whereas the skeletal flexibility enables it to adopt different adsorption geometries, with its feet on different surface atoms.

Periodic density functional theory (DFT) calculations of **2** on the Cu(110) surface confirmed that it adopts the horseshoe conformation, in which the phenyl ring is held up away from the surface and the molecule stands on its two imidazolyl feet that are held to the surface by chemisorption between the two pyridyl-like N atoms and the surface Cu atoms (Figure 1 iii). In this stance, it has several stable geometries with binding energies ranging from 325 to 348 kJ mol^{-1} (see the Supporting Information, Figure S1). The two most favorable ones, with identical adsorption energies of 348 kJ mol^{-1}, are achieved when the feet are adsorbed on the same close-packed Cu row, separated by either four or three Cu atomic distances (a_0), which are labelled as the extended and contracted conformations, respectively, in Figure 1 iii. STM images of **2** obtained when diffusion is arrested at either low temperatures or when the walker molecule is trapped between fences consistently show a three-lobed structure, with two lobes aligned along the close-packed [1$\bar{1}$0] direction (Figure 1 iv). This experimental STM image is closely matched by the simulated STM image of **2** adsorbed with its feet three Cu atoms apart (Figure 1 iv), with the three imaged lobes corresponding to the three aromatic rings.

When **2** was deposited on the Cu(110) surface, long, straight, bright lines traversing tens of nanometers were observed at 135 K, suggesting unhindered and strongly anisotropic motion along the close-packed [1$\bar{1}$0] direction (Figure 2 i). Changing the STM scanning direction did not affect the appearance of the diffusion tracks, eliminating the possibility of tip-induced motion. The diffusion lines possess dimensions far larger than those of **2** (imaged as approximately 1 nm long and 0.8 nm wide, Figure 1 iv), indicating fast directional motion of the molecules relative to the timescale of the STM scanning process.

For confined motion, oligomeric fences of **1** were preformed on the surface as barriers orthogonal to the walker's diffusion direction (Figure 1 i and Figure 2 i, inset). After deposition of **2** onto the fence-strewn surface, STM images

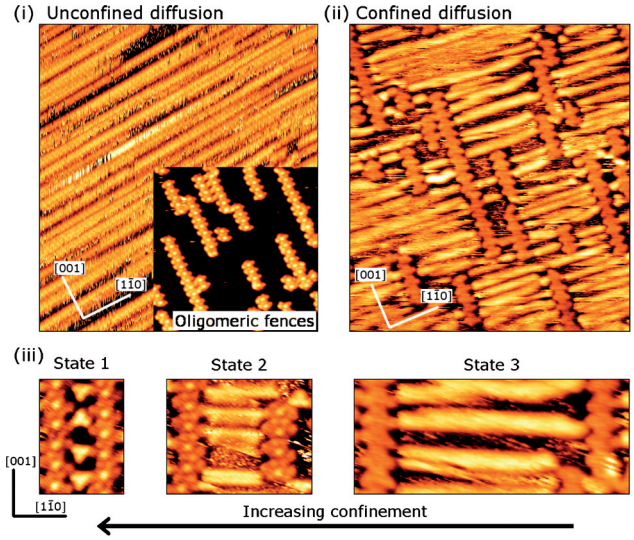

Figure 2. i) A representative STM image at 135 K of **2** diffusing on the Cu(110) surface (34.4×41.7 nm^2, $I(t) = -0.21$ nA, $V(t) = -390$ mV). Inset: Room-temperature STM image of fences of **1** (21.6×23.7 nm^2, $I(t) = -0.12$ nA, $V(t) = -1360$ mV). ii) A representative room-temperature STM image of **2** diffusing between fences of **1**, created by first forming fences on Cu(110), with **2** deposited subsequently (33.1×40.0 nm^2, $I(t) = 0.32$ nA, $V(t) = 780$ mV). Images remain unchanged when the STM scanning direction is altered. Coordinates apply to the inset of (i) as well. iii) Three close-up room-temperature STM images of **2** in between fences of **1** that are placed at different distances with respect to each other, leading to different degrees of confinement (State 1: 5.8×7.1 nm^2, $I(t) = -0.18$ nA, $V(t) = -1250$ mV; State 2: 8.2×7.1 nm^2, $I(t) = -0.18$ nA, $V(t) = -1200$ mV; State 3: 15.5×7.1 nm^2, $I(t) = 0.32$ nA, $V(t) = 780$ mV). Coordinates apply to all three states.

obtained at room temperature showed the original immobile lines of linked porphyrins and, between them, bright lines corresponding to a high tunneling current (Figure 2ii). These lines were always found to be perpendicular to the fences, demonstrating that the movement of **2** is still predominantly occurring in the [1$\bar{1}$0] direction. In the images and movies (see Figures S2, S3), there are no indications that the mobile walker can jump onto or over the fences; the fences are always imaged clearly, without any static molecules **2** nor noise corresponding to motion of **2** on top. Hence, we are witnessing constrained surface Brownian motion in one dimension dictated by the interaction of the walker with the surface and confined by the fences.

Clearly, the walker's mobility is restricted by the fences, which are separated from one another at random distances and located at random positions on the surface. Depending upon where the fences happen to be located, the walkers have free straight paths of various lengths to travel along, as seen in the large-area image in Figure 2ii. More detail on the diffusion behavior as the confinement is increased is shown in Figure 2iii.

When the fences are so close to each other that perpendicular diffusion of a potentially dynamic molecule is not possible, the latter is trapped and can be imaged individually by STM as a three-lobe structure (State 1 in Figure 2iii). When the chains are a little further apart, so that the interspersed surface space increases by a few atomic distances, then the walker starts to diffuse between the porphyrins (State 2). In such restricted spaces, the diffusion lines often show different intensity patterns corresponding to different residence times of the walker in a given region. For example, the middle two diffusion tracks in State 2 (Figure 2iii) show enhanced intensity close to the fences, suggesting a greater residence time of the walker near the fences. As the distance between the fences is increased, the diffusion of the walker is lengthened accordingly (State 3).

Under certain conditions, diffusion of **2** can be hindered, allowing for the imaging of individual molecules. When a large number of fences are present on the surface, akin to State 2 above, cooling to low temperature arrests the motion of the walker and the diffusion tracks disappear with individual "frozen" walker molecules imaged between the fences (see Figure S4). At room temperature, **2** is also occasionally imaged next to the long edge of the fence without being trapped, suggesting that a locally favorable adsorption site is hindering its diffusion (see Figure S3). Furthermore, there seem to be favorable interactions with the short edge of the fence, which can temporarily trap the walkers if they diffuse past in close proximity at room temperature (Figure 3i). This effect is especially strong if two

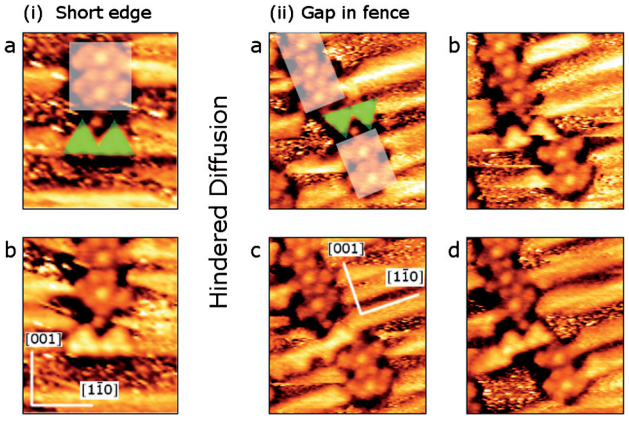

Figure 3. i) Two 4.8×5.5 nm^2 room-temperature STM images of two molecules **2** trapped temporarily at the short edge of a fence of **1** (a: $I(t) = -0.15$ nA, $V(t) = -1200$ mV; b: $I(t) = -0.19$ nA, $V(t) = -1200$ mV). Coordinates apply to both images. ii) Four subsequent 6.9×8.5 nm^2 STM images of multiple molecules of **2** moving through a small gap of approximately 1.5 nm in between two chains of **1** (a: $I(t) = -0.16$ nA, $V(t) = -1200$ mV; b: $I(t) = -0.17$ nA, $V(t) = -1200$ mV; c: $I(t) = -0.20$ nA, $V(t) = -1200$ mV; d: $I(t) = -0.18$ nA, $V(t) = -1200$ mV). Coordinates apply to all images. The locations of the chains and the two walker molecules are highlighted in the first images of (i) and (ii).

fences are close together in the [001] direction, providing small openings which the walker can diffuse through. For example, **2** can pass through gaps in the fence as small as 1.5 nm, albeit at a significantly reduced rate (Figure 3ii). In figurative terms, these spaces between fences act like turnstiles for the walkers.

In light of these results and to understand how **2** can diffuse on the surface, nudged elastic band calculations were

carried out to bridge various adsorption geometries along a given travel path. The diffusion of several starting conformations was studied in detail (see Figures S5–S9), including the most favorable one in which **2** has both feet on the same row (Figure 1 iii). Dynamic modelling reveals that the lowest diffusion barriers occur when **2** adopts its most favored conformations with both feet on the same surface row and walks along it with an inchworm motion (Figure 4 i), involving a low energy barrier of only 16 kJ mol^{-1}. Specific aspects of this walk (Figure 4 i) are that first, starting from the energetically favored extended conformation, **2** moves its rear "leg" to the nearest Cu atom along the row, forming a higher-energy transient structure with its legs three Cu atomic distances apart, before relaxing into the almost equally favored contracted conformation. Then, the front leg steps forward by bonding to the nearest Cu atom, again yielding a higher-energy transient structure, before forming the final extended configuration, which is equivalent to the initial one, but has moved by one surface atom. During the diffusion process, the Cu atoms are displaced by no more than 0.001 nm. The transition from the extended to the contracted conformation (or vice versa) requires breaking one N–Cu bond and moving the leg to the adjacent Cu atom, where a new N–Cu bond is formed, and **2** assumes a transitional conformation that is approximately 12–16 kJ mol^{-1} higher in energy before relaxing to the appropriate favored conformation. The evolution of electron density during a bond-breaking process is shown in Figure 4 i. The conformational flexibility of the walker and the match of its molecular dimensions to the underlying surface ensure that this walking process is not energetically expensive if carried out along the close-packed [1$\bar{1}$0] direction. The probabilities of the front leg or the rear leg moving first in opposite directions are identical, so forward and backward overall motion can occur equally.

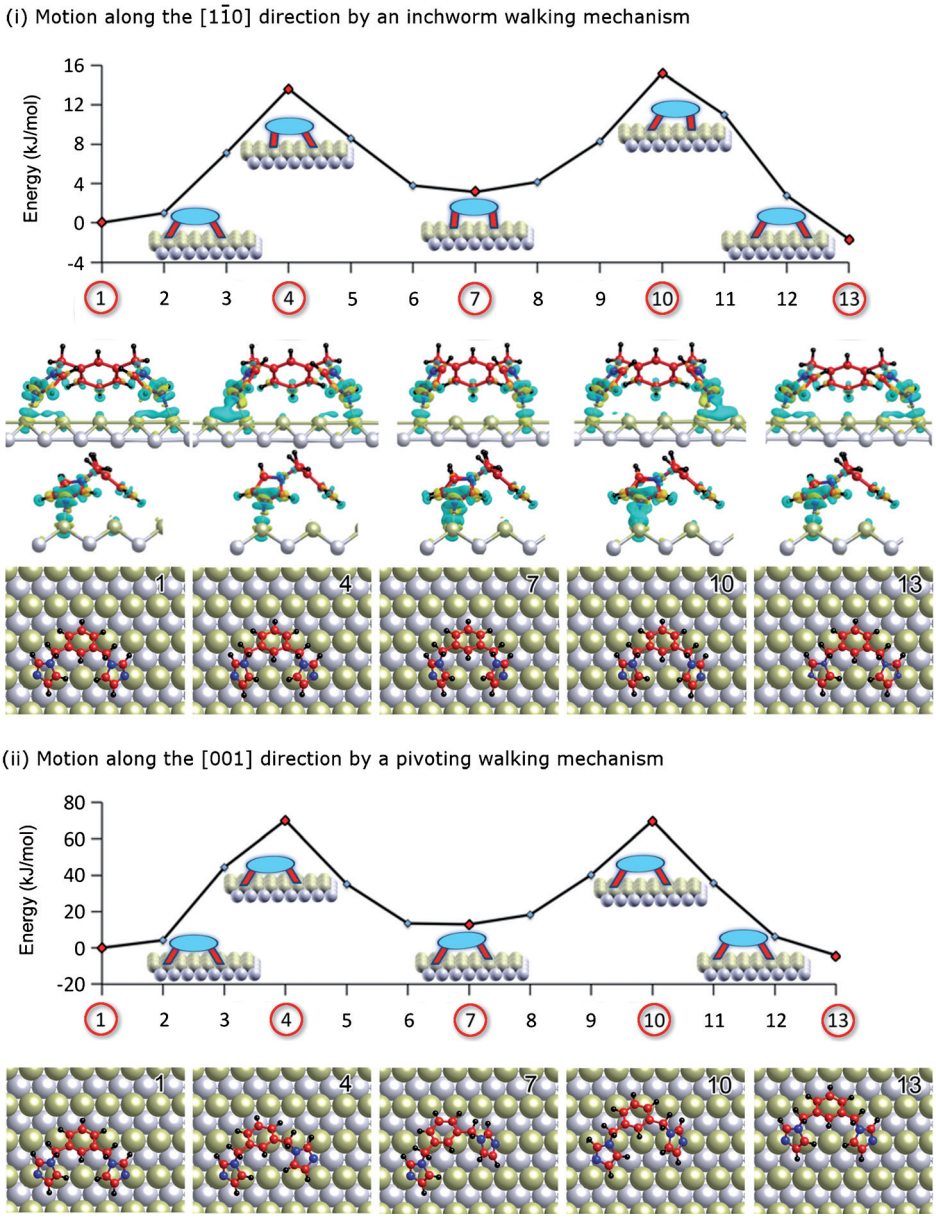

Figure 4. i) The DFT calculated minimum-energy path and the corresponding front, side, and top views of the selected geometries for **2** to diffuse one lattice constant a_0 along the Cu row between two equivalent extended structures. The molecule first steps with its rear leg towards its front one to the nearest Cu atom (points 1 to 7) to arrive at the contracted geometry, which is followed by the front leg to make another step by a_0 in the same direction to arrive at an equivalent (but shifted by a_0) extended geometry (points 7 to 13). ii) The DFT calculated minimum-energy path, and the corresponding top views of the selected geometries for **2** to diffuse one lattice constant b_0 perpendicular to the Cu row between two equivalent extended structures. The molecule first pivots on its rear leg to get the front leg onto the next row (points 1 to 7), then it pivots on the front leg to get the rear leg across (points 7 to 13). Charge density difference plots are shown for all selected structures in (i) using the same color scheme as in Figure 1.

Diffusion of the walker in the perpendicular [001] direction is performed in two steps using each of its legs as a pivot. It involves barriers at least four times larger (Figure 4 ii), explaining why jumps of the molecule between neighboring tracks are rare. This anisotropy in diffusion is the basis for the directional motion that is observed in the experiment. When either walking or pivoting, **2** breaks only

one bond at a time to reduce the overall energy barrier. Calculations show that diffusion undertaken in one step by sliding, where both legs are detached simultaneously, would invoke barriers that are at least two times larger than that of the equivalent walking motion. Walking mechanisms from less favorable starting positions and/or with greater diffusion barriers are shown in Figures S7 and S8.

The dynamic modelling agrees with the experimental observations of preferred diffusion along the rows, with the rate in the orthogonal direction calculated to be at least 10^5 times smaller at room temperature. This selectivity in the direction of diffusion is due to the specific manner in which the molecule binds to the copper and the anisotropic structure of the surface, leading to different barriers for motion in orthogonal paths. The inchworm mechanism is derived from the theoretical modelling; direct experimental evidence for this mechanism will require ultra-low-temperature STM measurements where the two conformations can be frozen and resolved at the submolecular level, and their evolution from one to the other captured. Furthermore, mean-square displacements of molecules, determined at a variety of temperatures, should yield diffusion barriers for comparison with theory.

In conclusion, a simple molecule can walk on a preferred path on a surface, with its motion effectively restricted by fences that are synthesized on the surface and aligned perpendicularly to the walking direction. This minimalist walker shuttles between the fences along the close-packed metallic rows, which act as intrinsic and directional tracks on the corrugated Cu(110) substrate. DFT modelling shows that the directionality of the motion arises from the specific interactions of the walker with the surface, which moves by attaching and detaching its imidazolyl feet in an inchworm fashion, and from anisotropic diffusion barriers. Thus, an anisotropic surface such as Cu(110) is an advantageous medium for molecular machines, used by others in other contexts,[13–18] with inherent structural features providing tracks along which molecules could be confined to shuttle. We note that the porphyrin framework can be readily functionalized, bringing prospects for creating non-equivalent "stations" for the walker to traverse between, and for engineering specific recognition of the shuttling molecule at either or both stations. Our system operates under thermal activation (room temperature is sufficient here), but it is also conceivable that systems could be designed where shuttling is initiated by an electrical pulse or light activation, for example, where aspects such as microscopic reversibility[19] could be studied at the submolecular level. Finally, dissymmetry in the walker mobility could lead to unidirectional motion. We are presently working towards these targets.

Keywords: diffusion · molecular machines · nanomaterials · scanning tunneling microscopy · surface chemistry

How to cite: *Angew. Chem. Int. Ed.* **2015**, *54*, 7101 – 7105
Angew. Chem. **2015**, *127*, 7207 – 7211

[1] M. von Delius, D. A. Leigh, *Chem. Soc. Rev.* **2011**, *40*, 3656 – 3676.
[2] A. Coskun, M. Banaszak, R. D. Astumian, J. F. Stoddart, B. A. Grzybowski, *Chem. Soc. Rev.* **2012**, *41*, 19 – 30.
[3] a) D. J. G. Bakewell, D. V. Nicolau, *Aust. J. Chem.* **2007**, *60*, 314 – 332; b) S. S. Patel, I. Donmez, *J. Biol. Chem.* **2006**, *281*, 18265 – 18268.
[4] a) D. Lensen, J. A. A. W. Elemans, *Soft Matter* **2012**, *8*, 9053 – 9063; b) S. Ishihara, Y. Wakayama, N. Hiroshiba, J. P. Hill, K. Ariga, *Curr. Org. Synth.* **2012**, *9*, 428 – 438; c) J. Puigmartí-Luis, W. J. Saletra, A. González, D. B. Amabilino, L. Pérez-García, *Chem. Commun.* **2014**, *50*, 82 – 84; d) J. Berná, D. A. Leigh, M. Lubomska, S. M. Mendoza, E. M. Perez, P. Rudolf, G. Teobaldi, F. Zerbetto, *Nat. Mater.* **2005**, *4*, 704 – 710.
[5] a) H. Hess, C. M. Matzke, R. K. Doot, J. Clemmens, G. D. Bachand, B. C. Bunker, V. Vogel, *Nano Lett.* **2003**, *3*, 1651 – 1655; b) K. Y. Kwon, K. L. Wong, G. Pawin, L. Bartels, S. Stolbov, T. S. Rahman, *Phys. Rev. Lett.* **2005**, *95*, 166101; c) Y. Makoudi, E. Arras, N. Kepčija, W. Krenner, S. Klyatskaya, F. Klappenberger, M. Ruben, A. P. Seitsonen, J. V. Barth, *ACS Nano* **2012**, *6*, 549 – 556.
[6] Y. Shirai, A. J. Osgood, Y. Zhao, K. F. Kelly, J. M. Tour, *Nano Lett.* **2005**, *5*, 2330 – 2334.
[7] T. Kudernac, N. Ruangsupapichat, M. Parschau, B. Macia, N. Katsonis, S. R. Harutyunyan, K. H. Ernst, B. L. Feringa, *Nature* **2011**, *479*, 208 – 211.
[8] D. Kühne, F. Klappenberger, W. Krenner, S. Klyatskaya, M. Ruben, J. V. Barth, *Proc. Natl. Acad. Sci. USA* **2010**, *107*, 21332 – 21336.
[9] a) M. T. Cuberes, R. R. Schlittler, J. K. Gimzewski, *Appl. Phys. Lett.* **1996**, *69*, 3016 – 3018; b) H. Shigekawa, K. Miyake, J. Sumaoka, A. Harada, M. Komiyama, *J. Am. Chem. Soc.* **2000**, *122*, 5411 – 5412.
[10] a) S. Haq, F. Hanke, M. S. Dyer, M. Persson, P. Iavicoli, D. B. Amabilino, R. Raval, *J. Am. Chem. Soc.* **2011**, *133*, 12031 – 12039; b) F. Hanke, S. Haq, R. Raval, M. Persson, *ACS Nano* **2011**, *5*, 9093 – 9103; c) S. Haq, F. Hanke, J. Sharp, M. Persson, D. B. Amabilino, R. Raval, *ACS Nano* **2014**, *8*, 8856 – 8870; in the present work, the linked native porphine was also used as the barrier and showed essentially the same behavior as the system described in the main text.
[11] S. Ramos, E. Alcalde, G. Doddi, P. Mencarelli, L. Perez-Garcia, *J. Org. Chem.* **2002**, *67*, 8463 – 8468.
[12] E. Alcalde, N. Mesquida, M. Alemany, C. Alvarez-Rua, S. Garcia-Granda, P. Pacheco, L. Perez-Garcia, *Eur. J. Org. Chem.* **2002**, 1221 – 1231.
[13] M. Schunack, T. R. Linderoth, F. Rosei, E. Laegsgaard, I. Stensgaard, F. Besenbacher, *Phys. Rev. Lett.* **2002**, *88*, 156102.
[14] R. Otero, Y. Naitoh, F. Rosei, P. Jiang, P. Thostrup, A. Gourdon, E. Laegsgaard, I. Stensgaard, C. Joachim, F. Besenbacher, *Angew. Chem. Int. Ed.* **2004**, *43*, 2092 – 2095; *Angew. Chem.* **2004**, *116*, 2144 – 2147.
[15] R. Otero, F. Hummelink, F. Sato, S. B. Legoas, P. Thostrup, E. Laegsgaard, I. Stensgaard, D. S. Galvao, F. Besenbacher, *Nat. Mater.* **2004**, *3*, 779 – 782.
[16] K. L. Wong, G. Pawin, K. Y. Kwon, X. Lin, T. Jiao, U. Solanki, R. H. J. Fawcett, L. Bartels, S. Stolbov, T. S. Rahman, *Science* **2007**, *315*, 1391 – 1393.
[17] S. C. Jensen, A. Shank, R. J. Madix, C. M. Friend, *ACS Nano* **2012**, *6*, 2925 – 2930.
[18] X. Bouju, F. Cherioux, S. Coget, G. Rapenne, F. Palmino, *Nanoscale* **2013**, *5*, 7005 – 7010.
[19] R. D. Astumian, *Nat. Nanotechnol.* **2012**, *7*, 684 – 688.

Received: March 6, 2015
Published online: April 29, 2015

